

Received: 2019.09.29
Accepted: 2019.11.05
Published: 2019.11.19

The Effects of Photobiomodulation on MC3T3-E1 Cells via 630 nm and 810 nm Light-Emitting Diode

Authors' Contribution:
Study Design A
Data Collection B
Statistical Analysis C
Data Interpretation D
Manuscript Preparation E
Literature Search F
Funds Collection G

ABCDEF 1 **Biao Chang**
AD 1 **Haixia Qiu**
AD 1 **Hongyou Zhao**
C 2,3 **Xi Yang**
AD 1 **Ying Wang**
B 1 **Tengda Ji**
CD 4,5,6 **Yuxuan Zhang**
CDEF 4,5,6 **Qi Quan**
B 1 **Yunqi Li**
BD 1 **Jing Zeng**
CD 4,5,6 **Haoye Meng**
AG 1 **Ying Gu**

1 Department of Laser Medicine, Chinese People's Liberation Army General Hospital, Beijing, P.R. China
2 State Key Laboratory of Proteomics, National Center for Protein Sciences (Beijing), Beijing Institute of Lifeomics, Beijing, P.R. China
3 General Hospital of Xinjiang Military Command, Urumqi, Xinjiang, P.R. China
4 Institute of Orthopedics, Chinese People's Liberation Army General Hospital, Beijing, P.R. China
5 Beijing Key Laboratory of Regenerative Medicine in Orthopedics, Beijing, P.R. China
6 Key Laboratory of Musculoskeletal Trauma and War Injuries, People's Liberation Army, Beijing, P.R. China

Corresponding Author: Ying Gu, e-mail: guyinglaser301@163.com

Source of support: This work was supported by the National Key R&D Program of China (2017YFB0403801)

Background: Photobiomodulation (PBM) has been explored as a promising therapeutic strategy to regulate bone cell growth; however, the effects of PBM on osteoblast cell lines remains poorly understood. In addition, as a light source of PBM, the light uniformity of light-emitting diode (LED) devices has not been given enough attention.

Material/Methods: Here, we sought to investigate the effects of PBM on MC3T3-E1 cells via 630 nm and 810 nm light from a newly designed LED with high uniformity of light. Cell proliferation, flow cytometric analysis, alkaline phosphatase (ALP) staining, ALP activity, Alizarin Red S staining, and quantitative real-time polymerase chain reaction (qRT-PCR) were carried out to assess treatment response. MC3T3-E1 cells were irradiated with LED devices (630±5 nm and 810±10 nm, continuous wave) for 200 seconds at a power density of 5 mW/cm² once daily.

Results: Increases in cell proliferation and decreases in cell apoptosis were evident following irradiation. ALP staining intensity and activity were also significantly increased following irradiation. Level of mineralization was obviously enhanced in irradiated groups compared with non-irradiated controls. qRT-PCR also showed significant increases in mRNA expression of osteocalcin (OCN) and osteoprotegerin (OPG) in the irradiated groups.

Conclusions: Our results showed that LED PBM could promote the proliferation, ALP staining intensity and activity, level of mineralization, gene expression of OCN and OPG of MC3T3-E1 cells, with no significant difference between the 630 nm- and 810 nm-irradiated groups.

MeSH Keywords: **Laser Therapy, Low-Level • Osteoblasts • Osteoporosis**

Abbreviations: **ALP** – alkaline phosphatase; **ATP** – adenosine triphosphate; **CCO** – cytochrome c oxidase; **GAPDH** – glyceraldehyde-3-phosphate dehydrogenase; **LED** – light-emitting diode; **OCN** – osteocalcin; **OPG** – osteoprotegerin; **PBM** – photobiomodulation; **PBS** – phosphate buffered saline; **ROS** – reactive oxygen species; **RT-PCR** – real-time polymerase chain reaction

Full-text PDF: <https://www.medscimonit.com/abstract/index/idArt/920396>

 3086

 2

 6

 58



Background

Osteoporosis, a common skeletal disease, can result in a greater propensity for fragility fracture [1–3]. Modulating the function of osteoblasts represents a promising therapeutic strategy for disease intervention as the combination of decreased osteoblastic activity and increased osteoclastic activity strongly contributes to the unbalanced bone metabolism underlying disease progression [3,4].

Photobiomodulation (PBM), also known as low-level laser therapy or low-level light therapy, is considered a promising new method for modulating osteoblasts, which play a key role in bone formation. PBM has demonstrated the capacity to promote tissue regeneration and reduce inflammation, swelling, and pain [5,6]. The wavelength is typically considered to be between 600 and 1000 nm [5,7]. Although the mechanisms of PBM are not well understood, it has been shown that cytochrome C oxidase (CCO), an enzyme in the mitochondrial oxidative respiratory chain, performs a vital role in light absorption. Stimulation of CCO can promote the photodissociation of inhibitory nitric oxide from CCO, increasing the synthesis of adenosine triphosphate (ATP), accompanied by the modulation of reactive oxygen species (ROS), ultimately leading to an upregulation of gene transcription. As a result, PBM has beneficial effects on cell respiration, especially for hypoxic cells. While the effects of PBM are not thermal in nature [5], temperature-gated calcium ion channels may be a target [8].

Red and infrared light was widely used in the study of PBM on osteoblasts, especially 630 nm and 810 nm light. Despite the significant promise of PBM, considerable disagreement persists regarding the ability of PBM to modulate the growth of osteoblasts [9]. Some studies had demonstrated that PBM could upregulate the proliferation and differentiation of several osteoblast cell lines [10–15]; however, these observations could not be replicated in all studies [16,17]. This divergence may be attributed to the different irradiation parameters used in different studies. The therapeutic effects of PBM depend on wavelength, power density, exposure time, energy density, and total energy. Use of continuous or pulsed wave treatments are also thought to affect treatment outcomes. Because these key parameters were not well described in some studies, some results cannot be properly evaluated.

Although laser, emitting coherent light, and light-emitting diode (LED), emitting non-coherent light, were both the light source of PBM [18], laser was more often used in the previous study [5,10–17]. There were more and more studies on PBM using LED [19–21]. Many studies supported that LED had similar reactions with laser [13,16–18,22,23]. LED is of many advantages compared with laser, it is more safety and cost-effective, easy to operation, can be used to irradiate large area at

once and made into wearable device [18]. However, the light emission angle of LED is much larger than laser, which determines the nonuniform power density in irradiation. As the light uniformity of LED is important for evaluating the effects of PBM, the power density in the irradiation region should be uniform. We designed a new LED device, by arranging the distribution of LEDs in the 2 sides of the edge, with a uniformity of power density >95%. In our study, we assessed the effects of PBM on MC3T3-E1 subclone 14 cells via newly designed 630 nm and 810 nm LED devices. Obviously enhanced proliferation and reduced apoptosis were found following irradiation. Alkaline phosphatase (ALP) staining intensity and activity were also significantly increased following irradiation. Compared with non-irradiated groups, calcium deposition was obviously increased in the irradiated groups. Finally, PCR revealed significant increases in osteogenic gene expression in the irradiated groups.

Material and Methods

Cell culture

The mouse MC3T3-E1 subclone 14 cells was provided by the Cell Bank of the Chinese Science Academy. MC3T3-E1 cells were cultivated in ascorbic acid-free MEM-a supplemented with 10% fetal bovine serum (Gibco, 10091148, CA, USA), 100 U/mL penicillin, and 100 U/mL streptomycin (Gibco, 10378016, CA, USA). Cells were sub-cultured using 0.25% trypsin (Gibco, 25200056, CA, USA) containing ethylenediaminetetraacetic acid after reaching 90% confluence.

To induce osteogenesis, osteogenic medium containing 50 µg/mL L-ascorbic acid (Sigma-Aldrich, 795437, St. Louis, MO, USA), 10 mM β-glycerophosphate (Sigma-Aldrich, G9422, St. Louis, MO, USA), and 10 nm dexamethasone (Sigma-Aldrich, D4902, St. Louis, MO, USA) was added. Medium and osteogenic factors were changed every 2 days.

LED irradiation

MC3T3-E1 cells were incubated in ascorbic acid-free culture medium for 24 hours, enabling cells to attach to the bottom of well, at which point the medium was changed to osteogenic medium, then cells were irradiated at 5 mW/cm² for 200 seconds every day with LED devices (630±5 nm and 810±10 nm, continuous wave), which were designed by the Institute of Semiconductors, Chinese Academy of Science. The irradiation parameters in detail was listed in Table 1. By arranging the distribution of LEDs in the 2 sides of the edge, the uniformities of power density of light within 6 cm of the center of the LED devices were >95% (Figure 1A). To test the effect of PBM on proliferation, cells were divided into a non-irradiated (control) group,

Table 1. Irradiation parameters.

Parameter	
Wavelength	630±5 nm, 810±10 nm
Wave type	Continuous wave
Power density	5 mW/cm ²
Application time	200 s
Energy density	1J/cm ²
Number of applications	1-time per day
Energy deposited per cm ²	1 J
Distance of irradiation to bottom of plate	5 cm

a 630 nm LED-irradiated group, and an 810 nm LED-irradiated group. To determine the effect of PBM on MC3T3-E1 differentiation, the non-irradiated group was subdivided into osteogenic and non-osteogenic (control) groups. The distance between the bottom of the cell culture plate and the irradiation surface of LED device was 5 cm (Figure 1B). The power density could be adjusted through a direct current power supply. The power density was calibrated every time before irradiation using a spectral power density meter (SENSING, SPD-370, Zhejiang, China).

Cell proliferation assay

MC3T3-E1 cells were seeded in 96-well plates (2000 cells/per well). Cell viability was evaluated 1, 3, and 5 days after the first irradiation treatment using Cell Counting Kit-8 (Beyotime, C0039, Shanghai, China). The optical density was measured at 450 nm via an enzyme-linked immunosorbent assay (ELISA) plate reader (Bio Tek EPOCH TAKE 3, VT, USA).

Flow cytometric analysis

MC3T3-E1 cells were seeded in 6-well plates (4×10⁵ cells/well). Cell apoptosis was detected using an annexin V-FITC/propidium iodide (PI) kit (Beyotime, C1062, Shanghai, China). One day after irradiation, the cells were rinsed with phosphate-buffered saline (PBS) and harvested. After centrifugation at 1300×g for 3 minutes, 10⁵ cells were resuspended in 195 µL of annexin V-FITC binding buffer, then 5 µL annexin V-FITC and 10 µL PI were added. After incubation at room temperature for 20 minutes in the dark, the fluorescence of 10 000 events per sample were analyzed by flow cytometry (FACSCelesta; BD Biosciences, NJ, USA). Live cells (annexin V-/PI-), early apoptotic cells (annexin V+/PI-), and late apoptotic cells (annexin V+/PI+) were distinguished.

ALP staining

MC3T3-E1 cells were seeded in 24-well plates (8×10⁴ cells/well), incubated for 7 or 14 days after the first irradiation, and washed with PBS. Cells were fixed with citrate-acetone-formaldehyde

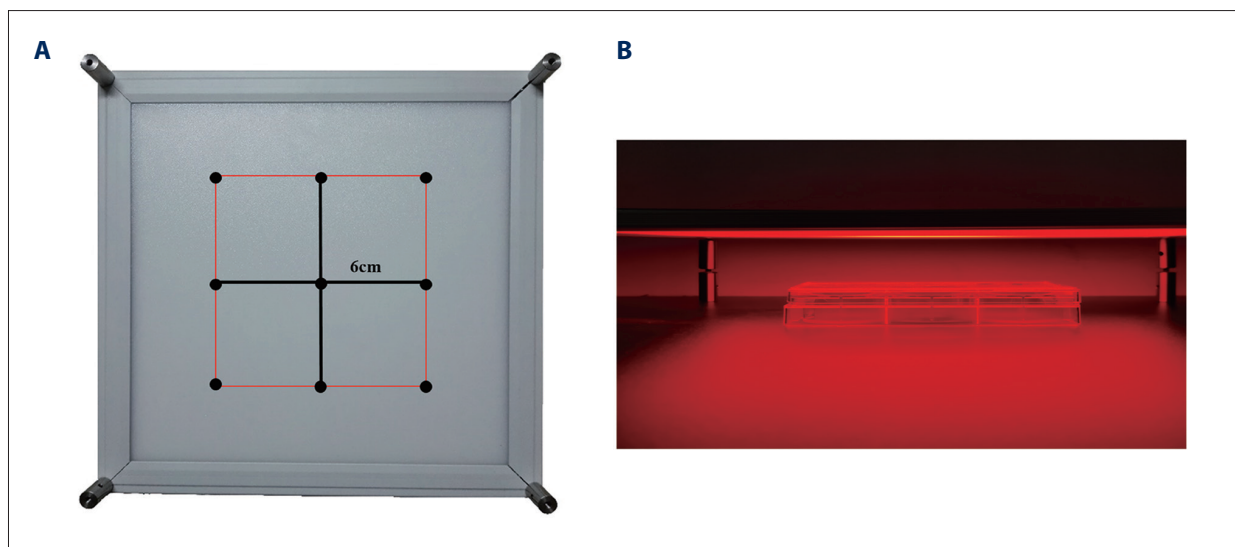


Figure 1. Overview of the light-emitting diode (LED) device. We arranged the distribution of many LED in the 2 sides of the edge and cover a glass in the irradiation surface to homogenize the light. (A) We measured the power density of 9 points in the interested field at a distance of 5 cm using a spectral power density meter.

$$\text{uniformity} = \frac{\text{power density (minimum)}}{\text{power density (maximum)}} \times 100\%$$

The uniformity of light within 6 cm of the center of the LED device was >95%. (B) Overview of the irradiation process.

fixative solution for 30 seconds and rinsed in deionized water for 60 seconds. The alkaline-dye mixture (Sigma-Aldrich, 86C, St. Louis, MO, USA) was prepared and incubated for 15 minutes. After incubation, cells were rinsed with deionized water for 120 seconds.

ALP activity assay

MC3T3-E1 cells were seeded in 6-well plates (4×10^5 cells/well), incubated for 7 or 14 days after the first irradiation, and washed with PBS. Cells were harvested in 100 μ L/well of lysis buffer (Beyotime, P0013), Shanghai, China) containing 20 mM Tris (pH 7.5), 150 mM NaCl, and 1% Triton X-100. Cells were centrifuged at 12 000 *g* for 5 min at 4°C, after which the supernatants were used for ALP activity evaluation using the Alkaline Phosphatase Assay Kit (Beyotime, P0321, Shanghai, China). Samples were read using an ELISA plate reader at 405 nm. ALP activity was normalized to the total intracellular protein content, which was determined by the Enhanced BCA Protein Assay Kit (Beyotime, P0010S, Shanghai, China), with samples read using an ELISA plate reader at 562 nm. ALP activity is presented as mU/mg protein.

Extracellular matrix mineralization assay

To evaluate extracellular matrix mineralization, Alizarin Red S (pH 4.2) staining solution (Solarbio, G1452, Beijing, China) was used. MC3T3-E1 cells were seeded in 24-well plates (8×10^4 cells/well), and cultured for 21 days after the first irradiation, after which cells were washed with PBS without calcium magnesium. Cells were then fixed with citrate-acetone-formaldehyde fixative solution for 30 seconds. After fixation, cells were washed with deionized water and stained with the Alizarin Red S staining solution for 30 minutes. The unbound stain was removed with deionized water. Semi-quantitative analysis of Alizarin Red S staining was evaluated by eluting the bound stain with 200 μ L of 10% cetyl-pyridinium chloride [8,24] in PBS for 2 hours at 37°C, as described previously [8,24]. To determine the amount of relative calcium deposition, the absorbance of 100 μ L eluted solution was measured using the ELISA plate reader at 562 nm.

Quantitative real-time polymerase chain reaction (qRT-PCR)

MC3T3-E1 cells were cultured for 21 days under the same conditions as that of the ALP activity assay. Twenty-one days after the first irradiation, cells were washed with PBS. RNA was collected and purified using the RiboPure Kit (Ambion, AM1924, USA) with the RNase/DNase-Free set. cDNA was synthesized from 1 μ g RNA with ReverTra Ace qPCR RT Master Mix (Toyobo, FSQ-201, Osaka, Japan) and treated as follows: 5 minutes heat denaturation at 65°C, 15 minutes reverse transcription at 37°C,

Table 2. Primers used for quantitative RT-PCR.

Gene	Sequence (5'→3')
GAPDH	F: CCAACTCTTTTGCCAGAGA
	R: GGCTACATTGGTGTGAGCTTTT
OCN	F: CTGACCTCACAGATCCCAAGC
	R: TGGTCTGATAGCTCGTCAAG
OPG	F: CCTGCCCTGACCACTCTTAT
	R: CACACACTCGTTGTGGGT

GAPDH – glyceraldehyde-3-phosphate dehydrogenase;
OCN – osteocalcin; OPG – osteoprotegerin.

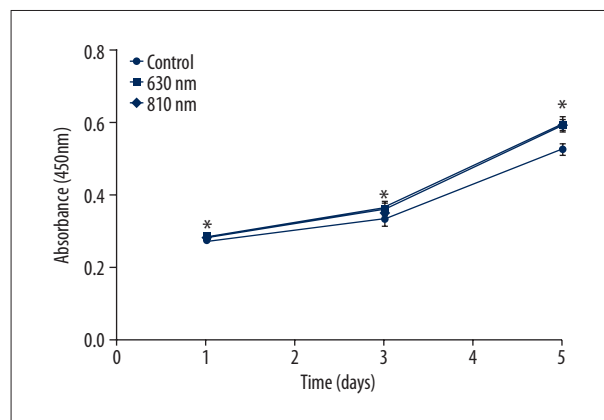


Figure 2. Effect of light-emitting diode (LED) photobiomodulation (PBM) on the proliferation of MC3T3-E1 cells. Cell viability assays were performed 1, 3, and 5 days after the first irradiation. * $P < 0.05$.

5 minutes inactivation at 98°C, and hold at 4°C. SYBR Green Realtime PCR Master Mix-Plus (Toyobo, QPK-212, Osaka, Japan) was used for PCR amplification, which was performed as follows: 60 seconds at 95°C, followed by 40 cycles of denaturation for 15 seconds at 95°C, annealing for 15 seconds at 60°C, and extension for 45 seconds at 72°C on a QuantStudio 7 Flex Real-Time PCR System (Applied Biosystems, Thermo Fisher Scientific, MA, USA). The primers were found in the primer bank (<https://pga.mgh.harvard.edu/primerbank/>). Primer sequences are shown in Table 2. The $2^{-\Delta\Delta Ct}$ method was used to quantify relative gene expression [25].

Statistical analysis

All data were reported as means \pm standard deviations of each group and were evaluated via ANOVA followed by the Student-Newman-Keuls post-hoc test. Differences were considered statistically significant at $P < 0.05$.

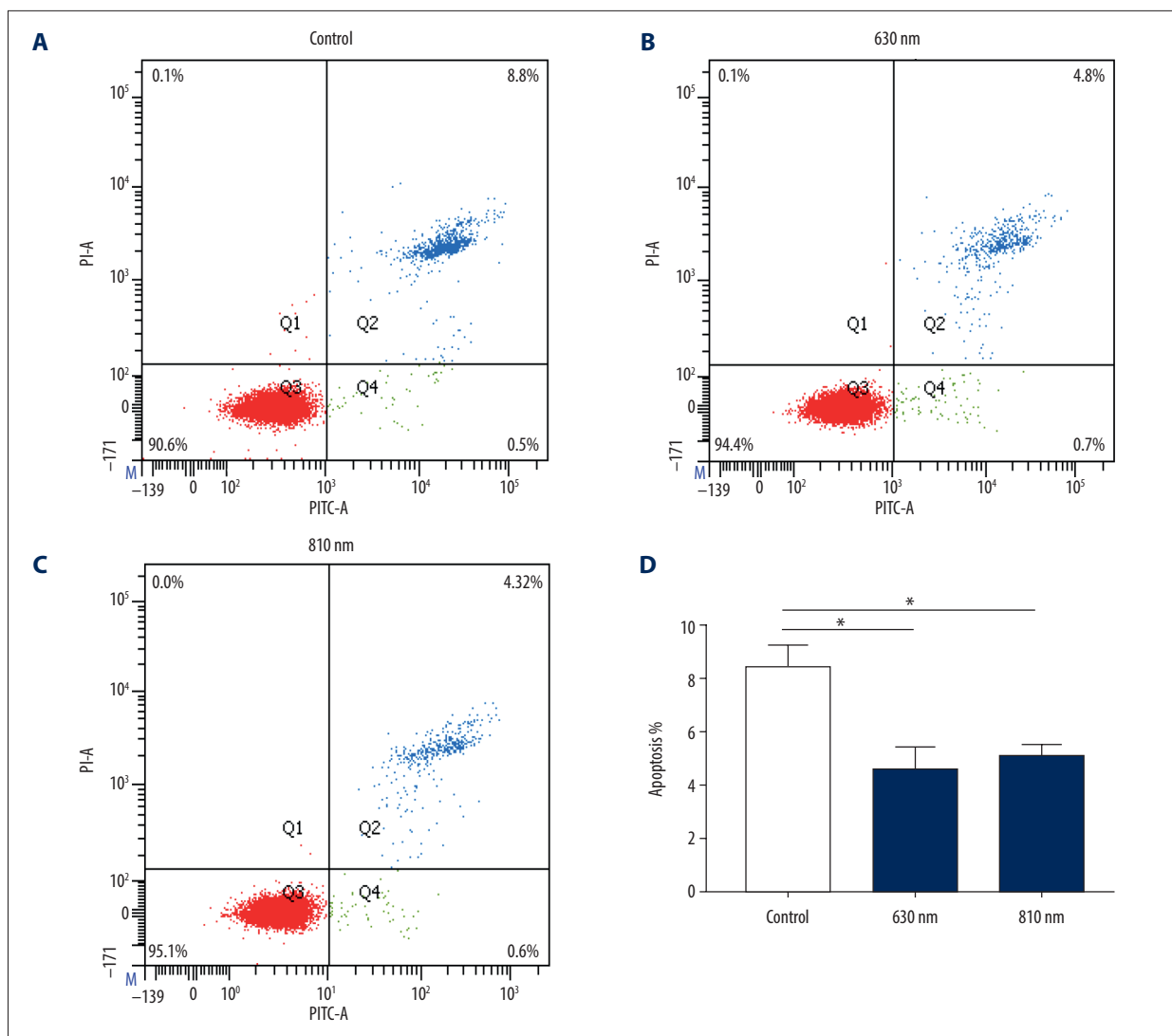


Figure 3. Effect of light-emitting diode (LED) photobiomodulation (PBM) on apoptosis of MC3T3-E1 cells. A representative histogram showing the distribution of annexin V and propidium iodide (PI)-labeled cells. Annexin V-/PI- (Q3) represented live cells, Annexin V+/PI- (Q4) represented early apoptotic cells, and annexin V+/PI+ (Q2) represented late apoptotic cells. (A) Control group. (B) 630 nm LED-irradiated group. (C) 810 nm LED-irradiated group. (D) A histogram depicting the percentage of apoptotic cells. Annexin V+/PI- (Q4)- and annexin V+/PI+ (Q2)-labeled cells were used for statistics. * $P < 0.05$.

Results

Effects of PBM on cell proliferation

The proliferation rate of MC3T3-E1 cells was significantly enhanced in the irradiated groups compared with non-irradiated controls from 1 to 5 days after the first irradiation, with no obvious difference between the 2 irradiated groups at any time point (Figure 2). Flow cytometric analysis showed that both 630 nm and 810 nm LED irradiation inhibited apoptosis of MC3T3-E1 cells (Figure 3). The results demonstrated that PBM had the capacity to promote proliferation and inhibit apoptosis in MC3T3-E1 cells.

Effects of LED PBM on ALP activity

ALP is an indicator of osteoblast differentiation. The addition of osteogenic medium significantly increased the intensity of ALP staining at 7 and 14 days. While the intensity of staining was higher in both the 630 nm- and 810 nm-irradiated groups, with similar effects between the 2 irradiated groups (Figure 4A). To better quantify these results, cells were examined using an ALP activity assay. The irradiated groups showed significantly higher ALP activity compared to non-irradiated groups, with similar effects seen between the 630 nm- and 810 nm-irradiated groups (Figure 4B). These results suggest that PBM may promote MC3T3-E1 cell differentiation.

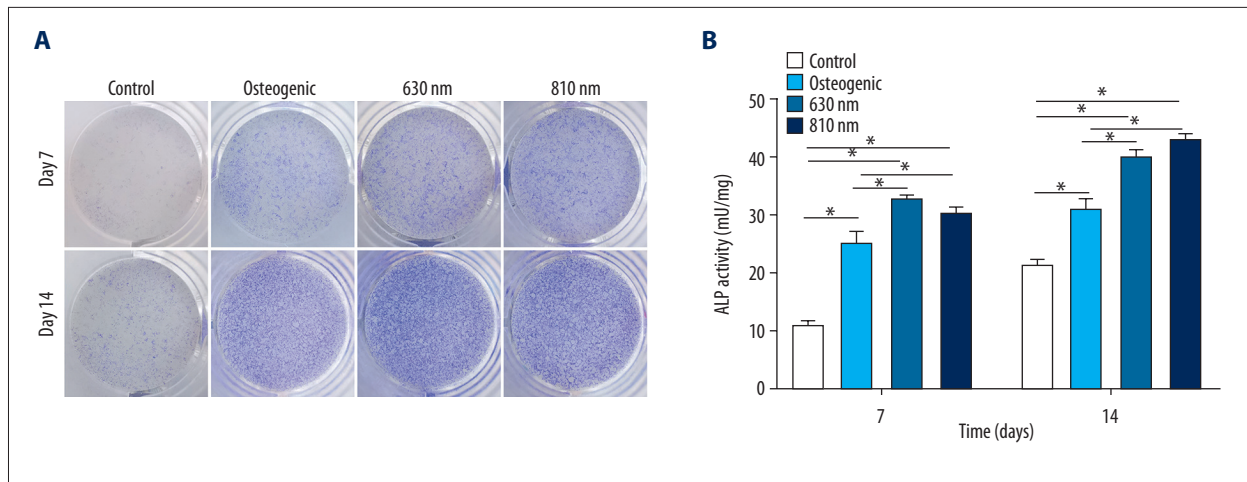


Figure 4. Effect of light-emitting diode (LED) photobiomodulation (PBM) on alkaline phosphatase (ALP) staining and activity in MC3T3-E1 cells. **(A)** ALP staining (blue), and **(B)** ALP activity after 7 and 14 days. ALP activity was normalized to total protein content and presented as mU/mg protein. * $P < 0.05$.

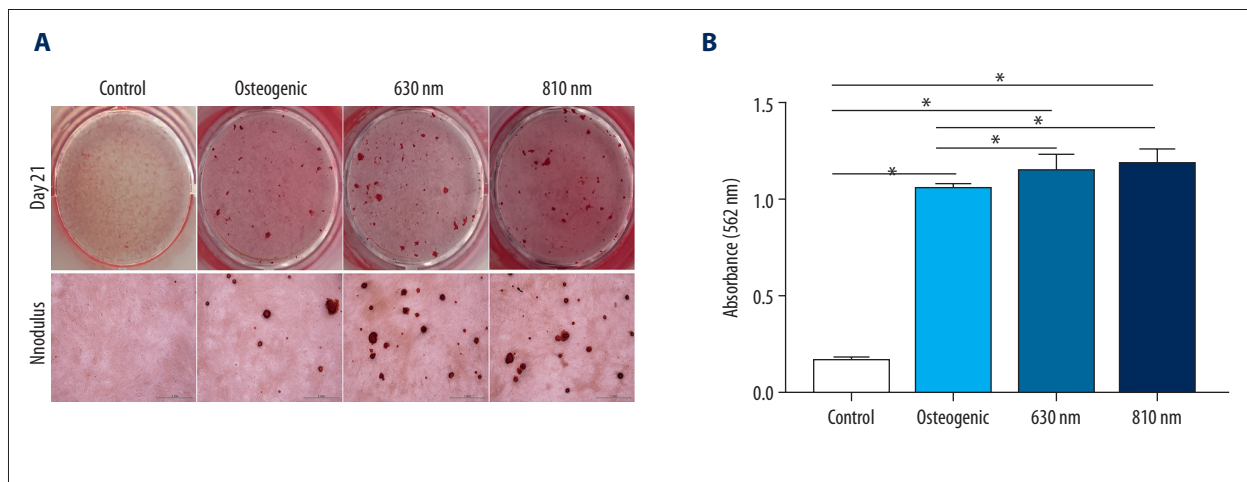


Figure 5. Effect of light-emitting diode (LED) photobiomodulation (PBM) on calcium deposition of MC3T3-E1 cells. **(A)** Calcium deposition was stained by Alizarin Red S and the calcium deposition nodules were stained red. Scale bar=1 mm. **(B)** Semi-quantitative analysis of calcium deposition. The absorption of eluate was measured at 562 nm. * $P < 0.05$.

Effects of LED PBM on extracellular matrix mineralization

Extracellular matrix mineralization results from calcium deposition and serves as a late marker of osteoblast differentiation. After 21 days, levels of Alizarin Red S staining indicated significant increases in calcification in both the osteogenic and irradiated groups; however, both the size and quantity of the calcifications in the irradiated groups were significantly greater than that of the osteogenic group (Figure 5A). To quantify the level of calcium deposition, we measured the absorbance of Alizarin Red S staining eluates at 562 nm. The absorbance was significantly higher in irradiated groups relative to non-irradiated controls, with similar levels of absorbance between the 2 irradiated groups (Figure 5B). These results indicated that PBM could facilitate extracellular matrix mineralization.

Effects of LED PBM on osteogenic gene expression

To confirm that PBM could promote differentiation of MC3T3-E1 cells, qRT-PCR was carried out to assess the effects of LED PBM on osteogenic gene expression. We examined the mRNA expression of osteocalcin (OCN) and osteoprotegerin (OPG), a key marker of late stage mineralization. OCN and OPG expressions were shown to be significantly increased in the irradiated groups compared to both the control and osteogenic groups, consistent with the idea that PBM could promote MC3T3-E1 cell differentiation (Figure 6). Unlike previous assays, for OCN, this effect was significantly greater in the 810 nm-irradiated group, relative to the 630 nm-irradiated group.

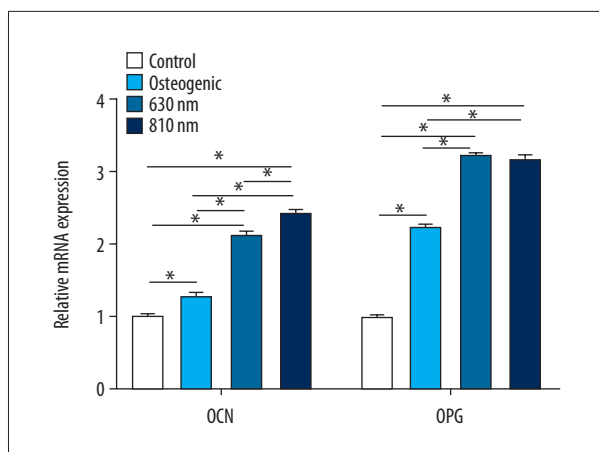


Figure 6. Effect of light-emitting diode (LED) photobiomodulation (PBM) on gene expression of MC3T3-E1 cells. Osteocalcin (OCN) and osteoprotegerin (OPG) expression was detected by quantitative real-time polymerase chain reaction (qRT-PCR) after 21 days. The $2^{-\Delta\Delta Ct}$ method was used to quantify relative gene expression. * $P < 0.05$.

Discussion

Osteoporosis is a common aging disease that affects 200 million people worldwide [26], which is characterized by an increased risk of fragility. Alleviating bone resorption and increasing bone formation is the most common strategy used to both treat and prevent osteoporosis [1,27]. Several drugs have been developed for this purpose, with most classified as either anabolic or antiresorptive [1,26,28–32], targeting osteoblasts and osteoclasts, respectively. Despite good overall therapeutic profiles, the use of these drugs may be impeded by low adherence and adverse effects.

As a non-invasive therapeutic method, PBM had been used to promote tissue regeneration, alleviate pain, and reduce inflammation [33–36]. In recent years, PBM received considerable attention due to its effects on osteoblast lines [10–14,16,17]. Red and near infrared light have been widely used in PBM for regulating bone cells. Numerous studies showed that red and near infrared light (630–810 nm) were able to increase proliferation, ALP staining and activity, calcium deposition, and osteogenic gene expression in several cell types [10–14,16,17,37,38], including bone marrow-derived mesenchymal stem cells, MC3T3-E1 cells, hypoxic-cultured human fetal osteoblasts, and human adipose-derived stem cells. Increased ATP synthesis accompanied by up-regulated ROS generation and transcription following PBM were shown to contribute to the proliferative effects [5]. Activation of Akt signaling may also mediate the osteogenic response of osteoblasts to red light [12]. Besides, activation of light-gated calcium ion channels may contribute to the promotive effects of 420 nm and 540 nm light in osteogenic differentiation [38].

Together, these studies provide strong evidence of a positive effect of PBM on osteogenic cell lines; however, contradictory findings have also been reported. Several studies have shown that PBM is not able to simultaneously promote proliferation and differentiation of osteoblast cells [12,16,17]. This inconsistent effect of PBM on osteoblasts has largely been attributed to differences in the parameters used in different studies. Of note, most studies showed that PBM could promote osteoblast proliferation and differentiation *in vitro*; similar effects have also been observed *in vivo*. Additional studies have also shown that PBM could increase the activity and density of osteoblasts [39,40].

Beyond its effects on osteoblasts, some studies have also demonstrated the potential of PBM to inhibit osteoclastogenesis [41,42]. Reduced ROS production has been proposed as a possible cause of reduced osteoclastogenesis following irradiation [41–43]. Moreover, many studies found that PBM could promote bone healing and improve bone quantity and strength in ovariectomized rats [39,40,44–46], in which near infrared light was more commonly used.

In recent years, LED had been widely used in other medical fields [19–21,47–51]. However, the light source of PBM in regulating osteoblasts was mainly focused on laser, and insufficient attention was paid to LED. The ultimate aim of studying the effect of LED PBM on osteoblasts was to treat osteoporosis. Although a previous study showed that 420 nm and 540 nm light was more effective than 660 nm and 810 nm light, due to the limitation of penetration depth [7], we did not choose on 420 nm and 540 nm light [38]. In our study, the effects of PBM on MC3T3-E1 cells were investigated using 630 nm and 810 nm LED lights.

The proliferation was obviously enhanced from 1 to 5 days following irradiation (Figure 2). In addition, the promotive effect was similar between the 2 irradiated groups. Meanwhile, PBM inhibited apoptosis of MC3T3-E1 cells, which might contribute to the enhanced cell viability (Figure 3). Increased proliferation and decreased apoptosis might facilitate osteogenic differentiation [52,53]. ALP, an indicative enzyme of osteoblast, was measured. The intensity of ALP staining was also significantly enhanced after irradiation relative to non-irradiated controls (Figure 4A). An ALP activity assay was further used to confirm these results, as these tests are more precise than ALP staining. Compared with non-irradiated groups, ALP activity was obviously enhanced in irradiated groups at all time points tested (Figure 4B), which gave more support to ALP staining. Calcium deposition, the indicative marker in the late stage of osteoblast differentiation, was evaluated by Alizarin Red S staining. We observed more red nodules in the irradiated groups compared to osteogenic groups (Figure 5A). Because the nodules were 3-dimensional with significant variations in size, we decided to elute the calcium deposits and measure

the absorbance of the eluates to quantify the level of mineralization. The higher absorbance in the irradiated groups confirmed that irradiation could significantly promote calcium deposition (Figure 5B). The enhanced mineralization levels were further supported by increases in OCN and OPG gene expression in the irradiated groups, relative to controls (Figure 6). Interestingly, the OCN expression was significantly higher in 810 nm irradiation group than 630 nm group, which might show the superiority of 810 nm light in promoting osteoblast differentiation. These results showed that LED PBM had promotive effects on MC3T3-E1 cells. The similar promotive effects between the 630 nm- and 810 nm-irradiated groups might attribute to the similar amount of photons absorption by CCO. Considering the deeper penetration depth [54,55], 810 nm light was more appropriate in studying PBM on osteoporosis *in vivo*.

In our study, we presented one dose effect of PBM on MC3T3-E1 cells. However, biphasic dose response was very common in the study of PBM [8,16,56,57]. The definition of dose was still controversial [5,58]. Power density, energy density, and total energy should be paid equal attention in the study of PBM.

References:

1. Rachner TD, Khosla S, Hofbauer LC: Osteoporosis: Now and the future. *Lancet*, 2011; 377: 1276–87
2. Ensrud KE, Crandall CJ: Osteoporosis. *Ann Intern Med*, 2017; 167: ITC17–32
3. Chang B, Quan Q, Li Y et al: Treatment of osteoporosis, with a focus on 2 monoclonal antibodies. *Med Sci Monit*, 2018; 24: 8758–66
4. Chang B, Quan Q, Lu S et al: The molecular mechanisms in the initiation phase of Wallerian degeneration. *Eur J Neurosci*, 2016; 44: 2040–48
5. Huang YY, Sharma SK, Carroll J, Hamblin MR: Biphasic dose response in low level light therapy – an update. *Dose Response*, 2011; 9: 602–18
6. Cotler HB, Chow RT, Hamblin MR, Carroll J: The use of low-level laser therapy (LLLT) for musculoskeletal pain. *MOJ Orthop Rheumatol*, 2015; 2(5): pii: 00068
7. Yun SH, Kwok SJJ: Light in diagnosis, therapy and surgery. *Nat Biomed Eng*, 2017; 1: 0008
8. Wang Y, Huang YY, Wang Y et al: Photobiomodulation of human adipose-derived stem cells using 810 nm and 980 nm lasers operates via different mechanisms of action. *Biochim Biophys Acta*, 2017; 1861: 441–49
9. Deana A, de Souza A, Teixeira V et al: The impact of photobiomodulation on osteoblast-like cell: A review. *Lasers Med Sci*, 2018; 33: 1147–58
10. Asai T, Suzuki H, Kitayama M et al: The long-term effects of red light-emitting diode irradiation on the proliferation and differentiation of osteoblast-like MC3T3-E1 cells. *Kobe J Med Sci*, 2014; 60: E12–18
11. Fallahnezhad S, Piryaei A, Darbandi H et al: Effect of low-level laser therapy and oxytocin on osteoporotic bone marrow-derived mesenchymal stem cells. *J Cell Biochem*, 2018; 119: 983–97
12. Tani A, Chellini F, Giannelli M et al: Red (635 nm), near-infrared (808 nm) and violet-blue (405 nm) photobiomodulation potentiality on human osteoblasts and mesenchymal stromal cells: A morphological and molecular *in vitro* study. *Int J Mol Sci*, 2018; 19(7): pii: E1946
13. Kim HK, Kim JH, Abbas AA et al: Red light of 647 nm enhances osteogenic differentiation in mesenchymal stem cells. *Lasers in Medical Science* 2009;24: 214–22.
14. Pyo SJ, Song WW, Kim IR, et al. Low-level laser therapy induces the expressions of BMP-2, osteocalcin, and TGF-beta1 in hypoxic-cultured human osteoblasts. *Lasers Med Sci*, 2013; 28: 543–50
15. Bayram H, Kenar H, Tasar F, Hasirci V: Effect of low level laser therapy and zoledronate on the viability and ALP activity of Saos-2 cells. *Int J Oral Maxillofac Surg*, 2013; 42: 140–46
16. Pagin MT, de Oliveira FA, Oliveira RC et al: Laser and light-emitting diode effects on pre-osteoblast growth and differentiation. *Lasers Med Sci*, 2014; 29: 55–59
17. Peng F, Wu H, Zheng Y et al: The effect of noncoherent red light irradiation on proliferation and osteogenic differentiation of bone marrow mesenchymal stem cells. *Lasers Med Sci*, 2012; 27: 645–53
18. Heiskanen V, Hamblin MR: Photobiomodulation: Lasers vs. light emitting diodes? *Photochem Photobiol Sci*, 2018; 17: 1003–17
19. Chan A, Lee T, Yeung M, Hamblin M: Photobiomodulation improves the frontal cognitive function of older adults. *Int J Geriatr Psychiatry*, 2019; 34: 369–77
20. de Paiva P, Casalechi H, Tomazoni S et al: Effects of photobiomodulation therapy in aerobic endurance training and detraining in humans: Protocol for a randomized placebo-controlled trial. *Medicine*, 2019; 98: e15317
21. Kobayashi F, Castelo P, Gonçalves M et al: Evaluation of the effectiveness of infrared light-emitting diode photobiomodulation in children with sleep bruxism: Study protocol for randomized clinical trial. *Medicine*, 2019; 98: e17193
22. Rosa CB, Habib FA, de Araujo TM et al: Laser and LED phototherapy on mid-palatal suture after rapid maxilla expansion: Raman and histological analysis. *Lasers Med Sci*, 2017; 32: 263–74
23. Tatmatsu-Rocha JC, Tim CR, Avo L et al: Mitochondrial dynamics (fission and fusion) and collagen production in a rat model of diabetic wound healing treated by photobiomodulation: Comparison of 904 nm laser and 850 nm light-emitting diode (LED). *J Photochem Photobiol B*, 2018; 187: 41–47
24. Lee DJ, Tseng HC, Wong SW et al: Dopaminergic effects on *in vitro* osteogenesis. *Bone Res*, 2015; 3: 15020
25. Livak KJ, Schmittgen TD: Analysis of relative gene expression data using real-time quantitative PCR and the 2(T)(-Delta Delta C) method. *Methods*, 2001; 25: 402–8
26. Cotts K, Cifu AS: Treatment of osteoporosis. *JAMA*, 2018; 319: 1040–41
27. Canalis E: Wnt signalling in osteoporosis: Mechanisms and novel therapeutic approaches. *Nat Rev Endocrinol*, 2013; 9: 575–83
28. Cosman F, de Beur SJ, LeBoff MS et al: Clinician's guide to prevention and treatment of osteoporosis. *Osteoporos Int*, 2014; 25: 2359–81
29. Kanis JA, McCloskey EV, Johansson H et al: European guidance for the diagnosis and management of osteoporosis in postmenopausal women. *Osteoporos Int*, 2013; 24: 23–57

The data presented here suggest that LED PBM might be a promising option for the management of osteoporosis. As light penetration depth is strongly influenced by the wavelength used [54,55], and is closely associated with therapeutic effects, further studies will be needed to identify the optimal wavelength and dose for therapeutic use.

Conclusions

In our study, we designed new LED devices to test the effects of PBM on MC3T3-E1 cells. Our results showed that LED PBM could promote the proliferation, ALP staining intensity and activity, level of mineralization, gene expression of OCN and OPG of MC3T3-E1 cells, with no significant difference between the 630 nm- and 810 nm-irradiated groups. LED PBM may therefore represent a promising strategy to modulate bone metabolism.

Conflict of Interest

None.

30. Cosman F: Anabolic and antiresorptive therapy for osteoporosis: Combination and sequential approaches. *Curr Osteoporos Rep*, 2014; 12: 385–95
31. Langdahl B, Libanati C, Crittenden D et al: Romosozumab (sclerostin monoclonal antibody) versus teriparatide in postmenopausal women with osteoporosis transitioning from oral bisphosphonate therapy: A randomised, open-label, phase 3 trial. *Lancet*, 2017; 390: 1585–94
32. Liu DB, Sui C, Wu TT et al: Association of bone morphogenetic protein (BMP)/Smad signaling pathway with fracture healing and osteogenic ability in senile osteoporotic fracture in humans and rats. *Med Sci Monit*, 2018; 24: 4363–71
33. Kim H, Choi JW, Kim JY et al: Low-level light therapy for androgenetic alopecia: A 24-week, randomized, double-blind, sham device-controlled multicenter trial. *Dermatol Surg*, 2013; 39: 1177–83
34. Bingol U, Altan L, Yurtkuran M: Low-power laser treatment for shoulder pain. *Photomed Laser Surg*, 2005; 23: 459–64
35. Ryden H, Persson L, Preber H, Bergstrom J: Effect of low level energy laser irradiation on gingival inflammation. *Swed Dent J*, 1994; 18: 35–41
36. Barikbin B, Khodamrdi Z, Kholoosi L et al: Comparison of the effects of 665 nm low level diode laser hat versus and a combination of 665 nm and 808 nm low level diode laser scanner of hair growth in androgenic alopecia. *J Cosmet Laser Ther*, 2017 [Epub ahead of print]
37. Mostafavinia A, Dehdehi L, Ghoreishi SK et al: Effect of *in vivo* low-level laser therapy on bone marrow-derived mesenchymal stem cells in ovariectomy-induced osteoporosis of rats. *J Photochem Photobiol B*, 2017; 175: 29–36
38. Wang Y, Huang YY, Wang Y et al: Photobiomodulation (blue and green light) encourages osteoblastic-differentiation of human adipose-derived stem cells: Role of intracellular calcium and light-gated ion channels. *Sci Rep*, 2016; 6: 33719
39. Re Poppi R, Da Silva AL, Nacer RS et al: Evaluation of the osteogenic effect of low-level laser therapy (808 nm and 660 nm) on bone defects induced in the femurs of female rats submitted to ovariectomy. *Lasers Med Sci*, 2011; 26: 515–22
40. Aras MH, Bozdag Z, Demir T et al: Effects of low-level laser therapy on changes in inflammation and in the activity of osteoblasts in the expanded premaxillary suture in an ovariectomized rat model. *Photomed Laser Surg*, 2015; 33: 136–44
41. Sohn HM, Ko Y, Park M et al: Comparison of the alendronate and irradiation with a light-emitting diode (LED) on murine osteoclastogenesis. *Lasers Med Sci*, 2017; 32: 189–200
42. Lim HJ, Bang MS, Jung HM et al: A 635-nm light-emitting diode (LED) therapy inhibits bone resorptive osteoclast formation by regulating the actin cytoskeleton. *Lasers Med Sci*, 2014; 29: 659–70
43. Sohn H, Ko Y, Park M et al: Effects of light-emitting diode irradiation on RANKL-induced osteoclastogenesis. *Lasers Surg Med*, 2015; 47: 745–55
44. Bayat M, Fridoni M, Nejati H et al: An evaluation of the effect of pulsed wave low-level laser therapy on the biomechanical properties of the vertebral body in two experimental osteoporosis rat models. *Lasers Med Sci*, 2016; 31: 305–14
45. Fridoni M, Masteri Farahani R, Nejati H et al: Evaluation of the effects of LLLT on biomechanical properties of tibial diaphysis in two rat models of experimental osteoporosis by a three point bending test. *Lasers Med Sci*, 2015; 30: 1117–25
46. Scalize PH, de Sousa LG, Regalo SC et al: Low-level laser therapy improves bone formation: Stereology findings for osteoporosis in rat model. *Lasers Med Sci*, 2015; 30: 1599–607
47. Sorbellini E, Rucco M, Rinaldi F: Photodynamic and photobiological effects of light-emitting diode (LED) therapy in dermatological disease: An update. *Lasers Med Sci*, 2018; 33: 1431–39
48. Han L, Liu B, Chen X et al: Activation of Wnt/ β -catenin signaling is involved in hair growth-promoting effect of 655-nm red light and LED in *in vitro* culture model. *Lasers Med Sci*, 2018; 33: 637–45
49. Joo H, Jeong K, Kim J, Kang H: Various wavelengths of light-emitting diode light regulate the proliferation of human dermal papilla cells and hair follicles via Wnt/ β -catenin and the extracellular signal-regulated kinase pathways. *Ann Dermatol*, 2017; 29: 747–54
50. Kim J, Woo Y, Sohn K et al: Wnt/ β -catenin and ERK pathway activation: A possible mechanism of photobiomodulation therapy with light-emitting diodes that regulate the proliferation of human outer root sheath cells. *Lasers Surg Med*, 2017; 49: 940–47
51. Choi S, Chang S, Biswas R et al: Light-emitting diode irradiation using 660 nm promotes human fibroblast HSP90 expression and changes cellular activity and morphology. *J Biophotonics*, 2019; 12: e201900063
52. Hock JM, Krishnan V, Onyia JE et al: Osteoblast apoptosis and bone turnover. *J Bone Miner Res*, 2001; 16: 975–84
53. Zou B, Shi Z, Wu Q, Chen G: The effect of 3-hydroxybutyrate on the *in vitro* differentiation of murine osteoblast MC3T3-E1 and *in vivo* bone formation in ovariectomized rats. *Biomaterials*, 2007; 28: 3063–73
54. Golovynskiy S, Golovynska I, Stepanova L et al: Optical windows for head tissues in near-infrared and short-wave infrared regions: Approaching transcranial light applications. *J Biophotonics*, 2018; 11: e201800141
55. Hemmer E, Benayas A, Legare F, Vetrone F: Exploiting the biological windows: Current perspectives on fluorescent bioprobes emitting above 1000 nm. *Nanoscale Horizons*, 2016; 1: 168–84
56. Gal P, Mokry M, Vidinsky B et al: Effect of equal daily doses achieved by different power densities of low-level laser therapy at 635 nm on open skin wound healing in normal and corticosteroid-treated rats. *Lasers Med Sci*, 2009; 24: 539–47
57. Skopin MD, Molitor SC: Effects of near-infrared laser exposure in a cellular model of wound healing. *Photodermatol Photoimmunol Photomed*, 2009; 25: 75–80
58. Huang YY, Chen AC, Carroll JD, Hamblin MR: Biphasic dose response in low level light therapy. *Dose Response*, 2009; 7: 358–83